10718 *Inorg. Chem.* **2010**, *49*, 10718–10726
DOI: 10.1021/ic1019197

Inorganic Chemistry
Article

Two-Dimensional, Pyrazine-Based Nonlinear Optical Chromophores with Ruthenium(II) Ammine Electron Donors

Benjamin J. Coe,*,† John Fielden,† Simon P. Foxon,† Inge Asselberghs,‡ Koen Clays,‡ and Bruce S. Brunschwig§

†*School of Chemistry, University of Manchester, Oxford Road, Manchester M13 9PL, U.K.,*
‡*Department of Chemistry, University of Leuven, Celestijnenlaan 200D, B-3001 Leuven, Belgium, and*
§*Molecular Materials Research Center, Beckman Institute, MC 139-74, California Institute of Technology, 1200 East California Boulevard, Pasadena, California 91125, United States*

Received September 20, 2010

Six new nonlinear optical (NLO) chromophores with pyrazinyl-pyridinium electron acceptors have been synthesized by complexing a known pro-ligand with electron donating $\{Ru^{II}(NH_3)_5\}^{2+}$ or *trans*-$\{Ru^{II}(NH_3)_4(py)\}^{2+}$ (py = pyridine) centers. These cationic complexes have been characterized as their PF_6^- salts by using various techniques including electronic absorption spectroscopy and cyclic voltammetry. The visible $d \rightarrow \pi^*$ metal-to-ligand charge-transfer (MLCT) absorptions gain intensity on increasing the number of Ru^{II} centers from one to two, but remain at constant energy. One or two $Ru^{III/II}$ redox processes are observed which are reversible, quasi-reversible, or irreversible, while all of the ligand-based reductions are irreversible. Molecular first hyperpolarizabilities β have been determined by using hyper-Rayleigh scattering (HRS) at 1064 nm, and depolarization studies show that the NLO responses of the symmetric species are strongly two-dimensional (2D) in character, with dominant "off-diagonal" β_{zyy} components. Stark (electroabsorption) spectroscopic measurements on the MLCT bands also allow the indirect determination of estimated static first hyperpolarizabilities β_0. Both the HRS and the Stark-derived β_0 values increase on moving from mono- to bimetallic complexes, and substantial enhancements in NLO response are achieved when compared with one-dimensional (1D) and 2D monometallic Ru^{II} ammine complexes reported previously.

Introduction

Various applications including advanced telecommunications and biological imaging may benefit from studies of organic nonlinear optical (NLO) materials.[1] After extensive research, the first such compound to become commercial is the salt (*E*)-4′-(dimethylamino)-*N*-methyl-4-stilbazolium tosylate (DAST), crystals of which can be used for terahertz (THz) wave generation via nonlinear frequency mixing (a quadratic NLO effect).[2] Molecular salts offer various attractive features, including tailorability of crystal structures via counterion metathesis; this aspect may be exploited to produce noncentrosymmetric materials which are required for bulk quadratic (second-order) NLO effects. Within the broad sweep of molecular NLO compounds, transition metal complexes are especially interesting because they allow desirable optical phenomena to be combined readily with redox, magnetic, and other properties.[3] To illustrate this point, a number of studies have exploited metal-based redox chemistry to reversibly switch various NLO effects.[4]

A parameter known as the first hyperpolarizability β is the origin of quadratic NLO effects at the molecular level, leading to the corresponding susceptibility $\chi^{(2)}$ in a solid when the bulk structure lacks centrosymmetry. Second harmonic generation (SHG) and linear electro-optic behavior are the most widely studied quadratic NLO effects. Large β values are characteristic of noncentrosymmetric and highly polarizable species, which typically contain strong electron donor and acceptor groups connected by an extended π-conjugated system. Molecules of this type also display intense $\pi \rightarrow \pi^*$ intramolecular charge-transfer (ICT) transitions that often occur in the visible region. As a consequence, experimentally measured β values are subject to resonance enhancement by

*To whom correspondence should be addressed. E-mail: b.coe@manchester.ac.uk.

(1) Selected general reviews: (a) *Molecular Nonlinear Optics: Materials, Physics and Devices*; Zyss, J., Ed.; Academic Press: Boston, 1994. (b) Bosshard, Ch.; Sutter, K.; Prêtre, Ph.; Hulliger, J.; Flörsheimer, M.; Kaatz, P.; Günter, P. Organic Nonlinear Optical Materials. In *Advances in Nonlinear Optics*; Gordon & Breach: Amsterdam, The Netherlands, 1995; Vol. *1*. (c) *Nonlinear Optics of Organic Molecules and Polymers*; Nalwa, H. S., Miyata, S., Eds.; CRC Press: Boca Raton, FL, 1997. (d) Marder, S. R. *Chem. Commun.* **2006**, 131. (e) *Nonlinear Optical Properties of Matter: From Molecules to Condensed Phases*; Papadopoulos, M. G., Leszczynski, J., Sadlej, A. J., Eds.; Springer: Dordrecht, 2006. (f) Kuzyk, M. G. *J. Mater. Chem.* **2009**, *19*, 7444.

(2) Selected examples: (a) Taniuchi, T.; Okada, S.; Nakanishi, H. *Appl. Phys. Lett.* **2004**, *95*, 5984. (b) Taniuchi, T.; Ikeda, S.; Okada, S.; Nakanishi, H. *Jpn. J. Appl. Phys.* **2005**, *44*, L652. (c) Schneider, A.; Neis, M.; Stillhart, M.; Ruiz, B.; Khan, R. U. A.; Günter, P. *J. Opt. Soc. Am. B* **2006**, *23*, 1822. (d) Schneider, A.; Stillhart, M.; Günter, P. *Opt. Express* **2006**, *14*, 5376. (e) Yang, Z.; Mutter, L.; Stillhart, M.; Ruiz, B.; Aravazhi, S.; Jazbinšek, M.; Schneider, A.; Gramlich, V.; Günter, P. *Adv. Funct. Mater.* **2007**, *17*, 2018. (f) McEntee, J. *Chemistry World*, March **2007**, pp 52−56.

 Published on Web 10/20/2010

variable degrees, and the elucidation of useful molecular structure−activity relationships necessitates deriving static (non-resonant) first hyperpolarizabilities β_0. The latter quantity is especially important for characterizing new chromophores because practical NLO applications must avoid any actual light absorption.

While the most widely studied NLO molecules are simple one-dimensional (1D) dipoles (e.g., the DAS^+ cation), multidimensional species such as two-dimensional (2D) dipoles are also of considerable interest.[5] Chromophores of this type may offer significant potential advantages over more traditional 1D species, such as increased NLO responses without paying the normal and undesirable price of decreased visible transparency. In V-shaped molecules, the presence of more than one significant component of the β tensor can be exploited to avoid reabsorption of photons produced via SHG that is polarized perpendicular to the ICT transition dipole moment (μ_{12}), and phase-matching between the fundamental and harmonic waves can also be facilitated.[5a]

Metal-based NLO chromophores most often contain electron-rich metal center(s), and their β responses are hence associated with metal-to-ligand charge-transfer (MLCT) transitions. Complexes of ruthenium are among the most popular and promising species in this field,[3k] and we have studied previously various 1D Ru^{II} ammine complexes of pyridinium-substituted ligands that show very large β_0 responses.[3i] Such compounds are prototypical redox-switchable systems.[6,4f] Related investigations have involved 2D, V-shaped complexes containing a $\{Ru^{II}(NH_3)_4\}^{2+}$ moiety connected to two pyridinium electron acceptors.[3i,7] Given that the strongest electron-withdrawing group we have used to date is the *N*-(2-pyrimidyl)pyridinium moiety,[8] related species containing isomeric pyrazinyl groups appear attractive. The compound 2,6-dichloropyrazine has been reacted recently with 4,4′-bipyridyl to produce a ligand for copper(II),[9] and this provides a precedent to access 2D pyridinium chromophores with Ru^{II} ammine centers. Here we describe several such new molecules that show promising quadratic NLO properties. To our knowledge, this work includes the first experimental NLO studies on polynuclear Ru^{II} ammine complexes.

Experimental Section

Materials and Procedures. Acetonitrile was dried over CaH_2 and distilled under N_2, and dry dimethylformamide (DMF) was obtained in SureSeal bottles from Sigma Aldrich. Water and acetone were degassed using argon before use in the synthesis of the Ru(II) complexes. All other reagents and solvents were obtained as ACS grade from Sigma Aldrich, Alfa Aesar, or Fisher Scientific and used as supplied. The complex salts $[Ru^{II}(NH_3)_5(H_2O)][PF_6]_2$[10] and *trans*-$[Ru^{II}(NH_3)_4(py)(H_2O)][PF_6]_2$ (py = pyridine)[11] were synthesized according to established methods. The aqueous NH_4PF_6 solution used to precipitate the products was about 20% w/v. All reactions were carried out under an atmosphere of dry argon. Products were dried at room temperature overnight in a vacuum desiccator ($CaSO_4$) prior to characterization.

General Physical Measurements. ^{1}H NMR spectra were recorded on Bruker UltraShield 500, AV-400 or DPX-300 spectrometers, and all shifts are quoted with respect to tetramethylsilane (TMS). The fine splitting of pyridyl or phenyl ring AA′BB′ patterns is ignored, and the signals are reported as simple doublets, with *J* values referring to the two most intense peaks. Abbreviations used: ax = axial; eq = equatorial. Elemental analyses were performed by the Microanalytical Laboratory, University of Manchester by using a Carlo Erba EA1108 instrument. UV−vis spectra were obtained by using a Shimadzu UV-2401 PC spectrophotometer, and mass spectra were recorded by using +electrospray on a Micromass Platform II spectrometer. Cyclic

(3) Recent reviews: (a) Le Bozec, H.; Renouard, T. *Eur. J. Inorg. Chem.* **2000**, 229. (b) Barlow, S.; Marder, S. R. *Chem. Commun.* **2000**, 1555. (c) Lacroix, P. G. *Eur. J. Inorg. Chem.* **2001**, 339. (d) Di Bella, S. *Chem. Soc. Rev.* **2001**, *30*, 355. (e) Goovaerts, E.; Wenseleers, W. E.; Garcia, M. H.; Cross, G. H. In *Handbook of Advanced Electronic and Photonic Materials and Devices*; Nalwa, H. S., Ed.; Academic Press: San Diego, 2001; Vol. *9*, pp 127−191. (f) Coe, B. J. In *Comprehensive Coordination Chemistry II*; McCleverty, J. A., Meyer, T. J., Eds.; Elsevier Pergamon: Oxford, U.K., 2004; Vol. *9*, pp 621−687. (g) Maury, O.; Le Bozec, H. *Acc. Chem. Res.* **2005**, *38*, 691. (h) Cariati, E.; Pizzotti, M.; Roberto, D.; Tessore, F.; Ugo, R. *Coord. Chem. Rev.* **2006**, *250*, 1210. (i) Coe, B. J. *Acc. Chem. Res.* **2006**, *39*, 383. (j) Thompson, M. E.; Djurovich, P. E.; Barlow, S.; Marder, S. In *Comprehensive Organometallic Chemistry III*; Crabtree, R. H., Mingos, D. M. P., Eds.; Elsevier: Oxford, U.K., 2006; Vol. *12*, pp 101−194. (k) Coe, B. J. In ref 1e, pp. 571−608. (l) Zhang, C.; Song, Y.-L.; Wang, X. *Coord. Chem. Rev.* **2007**, *251*, 111. (m) Andraud, C.; Maury, O. *Eur. J. Inorg. Chem.* **2009**, 4357. (n) Di Bella, S.; Dragonetti, C.; Pizzotti, M.; Roberto, D.; Tessore, F.; Ugo, R. *Top. Organomet. Chem.* **2010**, *28*, 1.

(4) Selected examples: (a) Asselberghs, I.; Clays, K.; Persoons, A.; McDonagh, A. M.; Ward, M. D.; McCleverty, J. A. *Chem. Phys. Lett.* **2003**, *368*, 408. (b) Sporer, C.; Ratera, I.; Ruiz-Molina, D.; Zhao, Y.-X.; Vidal-Gancedo, J.; Wurst, K.; Jaitner, P.; Clays, K.; Persoons, A.; Rovira, C.; Veciana, J. *Angew. Chem., Int. Ed.* **2004**, *43*, 5266. (c) Cifuentes, M. P.; Powell, C. E.; Morrall, J. P.; McDonagh, A. M.; Lucas, N. T.; Humphrey, M. G.; Samoc, M.; Houbrechts, S.; Asselberghs, I.; Clays, K.; Persoons, A.; Isoshima, T. *J. Am. Chem. Soc.* **2006**, *128*, 10819. (d) Samoc, M.; Gauthier, N.; Cifuentes, M. P.; Paul, F.; Lapinte, C.; Humphrey, M. G. *Angew. Chem., Int. Ed.* **2006**, *45*, 7376. (e) Dalton, G. T.; Cifuentes, M. P.; Petrie, S.; Stranger, R.; Humphrey, M. G.; Samoc, M. *J. Am. Chem. Soc.* **2007**, *129*, 11882. (f) Boubekeur-Lecaque, L.; Coe, B. J.; Clays, K.; Foerier, S.; Verbiest, T.; Asselberghs, I. *J. Am. Chem. Soc.* **2008**, *130*, 3286. (g) Wahab, A.; Bhattacharya, M.; Ghosh, S.; Samuelson, A. G.; Das, P. K. *J. Phys. Chem. B* **2008**, *112*, 2842.

(5) Selected examples: (a) Wortmann, R.; Krämer, P.; Glania, C.; Lebus, S.; Detzer, N. *Chem. Phys.* **1993**, *173*, 99. (b) Moylan, C. R.; Ermer, S.; Lovejoy, S. M.; McComb, I.-H.; Leung, D. S.; Wortmann, R.; Krämer, P.; Twieg, R. J. *J. Am. Chem. Soc.* **1996**, *118*, 12950. (c) Di Bella, S.; Fragalà, I.; Ledoux, I.; Diaz-Garcia, M. A.; Marks, T. J. *J. Am. Chem. Soc.* **1997**, *119*, 9550. (d) Wolff, J. J.; Längle, D.; Hillenbrand, D.; Wortmann, R.; Matschiner, R.; Glania, C.; Krämer, P. *Adv. Mater.* **1997**, *9*, 138. (e) Averseng, F.; Lacroix, P. G.; Malfant, I.; Lenoble, G.; Cassoux, P.; Nakatani, K.; Maltey-Fanton, I.; Delaire, J. A.; Aukauloo, A. *Chem. Mater.* **1999**, *11*, 995. (f) Hilton, A.; Renouard, T.; Maury, O.; Le Bozec, H.; Ledoux, I.; Zyss, J. *Chem. Commun.* **1999**, 2521. (g) Lacroix, P. G. *Eur. J. Inorg. Chem.* **2001**, 339. (h) Ostroverkhov, V.; Petschek, R. G.; Singer, K. D.; Twieg, R. J. *Chem. Phys. Lett.* **2001**, *340*, 109. (i) Di Bella, S.; Fragalà, I.; Ledoux, I.; Zyss, J. *Chem.−Eur. J.* **2001**, *7*, 3738. (j) Yang, M.-L.; Champagne, B. *J. Phys. Chem. A* **2003**, *107*, 3942. (k) Wortmann, R.; Lebus-Henn, S.; Reis, H.; Papadopoulos, M. G. *J. Mol. Struct.* (*Theochem*) **2003**, *633*, 217. (l) Cui, Y.-Z.; Fang, Q.; Huang, Z.-L.; Xue, G.; Yu, W.-T.; Lei, H. *Opt. Mater.* **2005**, *27*, 1571. (m) Rigamonti, L.; Demartin, F.; Forni, A.; Righetto, S.; Pasini, A. *Inorg. Chem.* **2006**, *45*, 10976. (n) Li, H.-P.; Han, K.; Tang, G.; Shen, X.-P.; Wang, H.-T.; Huang, Z.-M.; Zhang, Z.-H.; Bai, L.; Wang, Z.-Y. *Chem. Phys. Lett.* **2007**, *444*, 80. (o) Zrig, S.; Koeckelberghs, G.; Verbiest, T.; Andrioletti, B.; Rose, E.; Persoons, A.; Asselberghs, I.; Clays, K. *J. Org. Chem.* **2007**, *72*, 5855. (p) Liu, C.-G.; Qiu, Y.-Q.; Su, Z.-M.; Yang, G.-C.; Sun, S.-L. *J. Phys. Chem. C* **2008**, *112*, 7021. (q) Li, H.-P.; Han, K.; Tang, G.; Li, M.-X.; Shen, X.-P.; Huang, Z.-M. *Mol. Phys.* **2009**, *107*, 1597. (r) Muhammad, S.; Janjua, M. R. S. A.; Su, Z.-M. *J. Phys. Chem. C* **2009**, *113*, 12551. (s) Sergeyev, S.; Didier, D.; Boitsov, V.; Teshome, A.; Asselberghs, I.; Clays, K.; Vande Velde, C. M. L.; Plaquet, A.; Champagne, B. *Chem.−Eur. J.* **2010**, *16*, 8181.

(6) Coe, B. J.; Houbrechts, S.; Asselberghs, I.; Persoons, A. *Angew. Chem., Int. Ed.* **1999**, *38*, 366.

(7) Coe, B. J.; Foxon, S. P.; Harper, E. C.; Helliwell, M.; Raftery, J.; Swanson, C. A.; Brunschwig, B. S.; Clays, K.; Franz, E.; Garín, J.; Orduna, J.; Horton, P. N.; Hursthouse, M. B. *J. Am. Chem. Soc.* **2010**, *132*, 1706.

(8) (a) Coe, B. J.; Harris, J. A.; Asselberghs, I.; Persoons, A.; Jeffery, J. C.; Rees, L. H.; Gelbrich, T.; Hursthouse, M. B. *J. Chem. Soc., Dalton Trans.* **1999**, 3617. (b) Coe, B. J.; Jones, L. A.; Harris, J. A.; Sanderson, E. E.; Brunschwig, B. S.; Asselberghs, I.; Clays, K.; Persoons, A. *Dalton Trans.* **2003**, 2335.

(9) Sun, Y.-Q.; Zhang, J.; Chen, J.-L.; Yang, G.-Y. *Eur. J. Inorg. Chem.* **2004**, 3837.

(10) Curtis, J. C.; Sullivan, B. P.; Meyer, T. J. *Inorg. Chem.* **1983**, *22*, 224.

(11) Chang, J.-H. P.; Fung, E. Y.; Curtis, J. C. *Inorg. Chem.* **1986**, *25*, 4233.

voltammetric measurements were performed by using an Ivium CompactStat. A single-compartment cell was used with a silver/silver chloride reference electrode (3 M NaCl, saturated AgCl) separated by a salt bridge from a 2 mm disk glassy carbon working electrode and Pt wire auxiliary electrode. $[N(C_4H_9\text{-}n)_4]PF_6$ (Fluka) was used as the supporting electrolyte. Solutions containing about 10^{-3} M analyte (0.1 M electrolyte) were deaerated by purging with N_2. All $E_{1/2}$ values were calculated from $(E_{pa} + E_{pc})/2$ at a scan rate of 200 mV s^{-1}.

Synthesis of 2,6-Bis[4-(pyridin-4-yl)pyridinium-1-yl]pyrazine Hexafluorophosphate, [Bbpypz][PF$_6$]$_2$ (1). A mixture of 2,6-dichloropyrazine (500 mg, 3.36 mmol) and 4,4′-bipyridyl (1.06 g, 6.79 mmol) in dry DMF (2.5 mL) was heated at 120 °C with stirring for 18 h. After cooling to room temperature, the mixture was washed out of the flask with ethanol (10 mL), and the crude chloride salt (791 mg) was precipitated by addition of diethyl ether, filtered off, and washed with hot toluene. The solid was dissolved in methanol and aqueous NH_4PF_6 added to give a precipitate which was filtered off and washed with water to yield an off-white solid: 932 mg, 40%; δ_H (400 MHz, $(CD_3)_2CO$) 10.15 (2 H, s, $C_4H_2N_2$), 10.12 (4 H, d, J = 6.6 Hz, C_5H_4N), 9.04 (4 H, d, J = 7.1 Hz, C_5H_4N), 8.97 (4 H, d, J = 6.1 Hz, C_5H_4N), 8.17 (4 H, d, J = 6.1 Hz, C_5H_4N). Anal. Calcd (%) for $C_{24}H_{18}F_{12}N_6P_2\cdot H_2O$: C, 41.27; H, 2.89; N, 12.03. Found: C, 41.62; H, 2.70; N, 11.86. m/z = 535.2 ([M − PF_6]$^+$), 195.1 ([M − 2PF_6]$^+$).

Synthesis of [{Ru^{II}(NH$_3$)$_5$}Bbpypz][PF$_6$]$_4$ (2) and [{Ru^{II}(NH$_3$)$_5$}$_2$-Bbpypz][PF$_6$]$_6$ (3). [Ru^{II}(NH$_3$)$_5$(H$_2$O)][PF$_6$]$_2$ (170 mg, 0.344 mmol) was added to a solution of **1**·H$_2$O (100 mg, 0.143 mmol) in degassed acetone (10 mL), resulting in an instantaneous color change to deep blue-green. The flask was protected from light, and the mixture stirred at room temperature for 18 h, then aqueous NH_4PF_6 (ca. 15 mL) was added, and the acetone removed under vacuum. After refrigeration for several hours, a dark blue precipitate (250 mg) was filtered off and washed with cold water. The products were separated by column chromatography on Sephadex CM-25 resin, using 5:3 mixtures of aqueous NaCl/acetone, with a 0.2−0.9 M concentration gradient of NaCl. The first major fraction contained [{Ru^{II}(NH$_3$)$_5$}Bbpypz]Cl$_4$, while the second contained the more highly charged complex in [{Ru^{II}(NH$_3$)$_5$}$_2$Bbpypz]Cl$_6$. These fractions were reduced in volume to about 10 mL under vacuum, before precipitation by addition of aqueous NH_4PF_6. The precipitates were filtered off, redissolved in 1:1 acetone/water, filtered and reprecipitated by addition of aqueous NH_4PF_6. Filtration and washing with cold water (ca. 5 mL) gave dark blue solids. **2**·3H$_2$O: 33 mg, 19%; δ_H (400 MHz, $(CD_3)_2CO$) 10.13 (2 H, s + s, separation ≈1 Hz, $C_4H_2N_2$), 10.11 (2 H, d, J = 7.8 Hz, C_5H_4N), 9.92 (2 H, d, J = 7.3 Hz, C_5H_4N), 9.29 (2 H, d, J = 7.1 Hz, C_5H_4N), 9.05 (2 H, d, J = 7.3 Hz, C_5H_4N), 9.01 (2 H, d, J = 7.3 Hz, C_5H_4N), 8.96 (2 H, d, J = 6.3 Hz, C_5H_4N), 8.15 (2 H, d, J = 6.3 Hz, C_5H_4N), 8.02 (2 H, d, J = 7.1 Hz, C_5H_4N), 3.91 (3 H, s, NH_3^{ax}), 2.82 (12 H, s, $4NH_3^{eq}$). Anal. Calcd (%) for $C_{24}H_{33}F_{24}N_{11}P_4Ru\cdot 3H_2O$: C, 23.81; H, 3.25; N, 12.73. Found: C, 23.93; H, 2.76; N, 12.45. **3**·4H$_2$O: 43 mg, 18%; δ_H (400 MHz, $(CD_3)_2CO$), 10.05 (2 H, s, $C_4H_2N_2$), 9.89 (4 H, d, J = 7.3 Hz, C_5H_4N), 9.28 (4 H, d, J = 7.1 Hz, C_5H_4N), 8.99 (4 H, d, J = 7.3 Hz, C_5H_4N), 8.01 (4 H, d, J = 7.0 Hz, C_5H_4N), 3.86 (6 H, s, $2NH_3^{ax}$), 2.78 (24 H, s, $8NH_3^{eq}$). Anal. Calcd (%) for $C_{24}H_{48}F_{36}N_{16}P_6Ru_2\cdot 4H_2O$: C, 16.91; H, 3.31; N, 13.15. Found: C, 17.26; H, 2.95; N, 12.70.

Synthesis of [{Ru^{II}(NH$_3$)$_5$}$_3$Bbpypz][PF$_6$]$_8$ (4). [Ru^{II}(NH$_3$)$_5$-(H$_2$O)][PF$_6$]$_2$ (220 mg, 0.445 mmol) was added to a solution of **1**·H$_2$O (50 mg, 0.072 mmol) in degassed acetone (20 mL), resulting in an instantaneous color change to deep blue-green. The flask was protected from light and the mixture stirred at room temperature for 18 h, then aqueous NH_4PF_6 (ca. 20 mL) was added and the acetone removed under vacuum. After refrigeration for several hours, a dark blue precipitate (144 mg) was filtered off and washed with cold water (ca. 5 mL). This solid was dissolved in acetone, filtered and aqueous NH_4PF_6 was added and the acetone removed under vacuum. Filtration and washing with cold water (ca. 5 mL) gave a dark blue solid: 100 mg, 63%; δ_H (400 MHz, $(CD_3)_2CO$) 10.15 (2 H, s, $C_4H_2N_2$), 9.67 (4 H, d, J = 7.1 Hz, C_5H_4N), 9.26 (4 H, d, J = 7.1 Hz, C_5H_4N), 8.90 (4 H, d, J = 7.3 Hz, C_5H_4N), 7.96 (4 H, d, J = 6.8 Hz, C_5H_4N), 4.36 (3 H, s, NH_3^{ax}), 3.86 (6 H, s, $2NH_3^{ax}$), 2.94 (12 H, s, $4NH_3^{eq}$), 2.80 (24 H, s, $8NH_3^{eq}$). Anal. Calcd (%) for $C_{24}H_{63}F_{48}N_{21}P_8Ru_3\cdot 0.25Me_2CO\cdot 6H_2O$: C, 13.32; H, 3.46; N, 13.18. Found: C, 13.18; H, 3.11; N, 12.71.

Synthesis of [{*trans*-Ru^{II}(NH$_3$)$_4$(py)}Bbpypz][PF$_6$]$_4$ (5) and [{*trans*-Ru^{II}(NH$_3$)$_4$(py)}$_2$Bbpypz][PF$_6$]$_6$ (6). *trans*-[Ru^{II}(NH$_3$)$_4$-(py)(H$_2$O)][PF$_6$]$_2$ (100 mg, 0.180 mmol) was added to a solution of **1**·H$_2$O (94 mg, 0.135 mmol) in degassed acetone (20 mL), resulting in an instantaneous color change to deep green. The flask was protected from light, and the mixture stirred at room temperature for 18 h, then aqueous NH_4PF_6 (ca. 20 mL) was added, and the acetone removed under vacuum. The dark blue precipitate (180 mg) was filtered off and washed with a small amount of cold water. The products were separated in manner similar to **2** and **3** by using a 0.1−0.8 M concentration gradient of NaCl, affording purple (**5**) and dark blue (**6**) solids. The latter (41 mg) was reprecipitated from acetone/diethyl ether. **5**·H$_2$O: 50 mg, 30%; δ_H (500 MHz, $(CD_3)_2CO$) 10.15 (1 H, s, $C_4H_2N_2$), 10.13 (2 H, d, J = 6.9 Hz, C_5H_4N), 10.11 (1 H, s, $C_4H_2N_2$), 10.01 (2 H, d, J = 7.3 Hz, C_5H_4N), 9.27 (2 H, d, J = 6.9 Hz, C_5H_4N), 9.07−9.03 (4 H, C_5H_4N), 8.98−8.94 (4 H, C_5H_4N + pyH^{2,6}), 8.21 (2 H, d, J = 6.9 Hz, C_5H_4N), 8.16 (2 H, d, J = 6.3 Hz, C_5H_4N), 8.02 (1 H, t, J = 7.6 Hz, pyH^4), 7.64 (2 H, t, J = 6.9 Hz, pyH^{3,5}), 2.92 (12 H, s, $4NH_3$). Anal. Calcd (%) for $C_{29}H_{35}F_{24}N_{11}P_4Ru\cdot H_2O$: C, 28.17; H, 3.02; N, 12.46. Found: C, 27.99; H, 2.58; N, 12.18. **6**·0.5Me$_2$-CO·H$_2$O: 25 mg, 10%; δ_H (500 MHz, $(CD_3)_2CO$) 10.09 (2 H, s, $C_4H_2N_2$), 10.00 (4 H, d, J = 6.9 Hz, C_5H_4N), 9.27 (4 H, d, J = 6.3 Hz, C_5H_4N), 9.04 (4 H, d, J = 6.9 Hz, C_5H_4N), 8.95 (4 H, d, J = 5.4 Hz, 2pyH^{2,6}), 8.22 (4 H, J = 6.3 Hz, C_5H_4N), 8.02 (2 H, t, J = 7.7 Hz, 2pyH^4), 7.64 (4 H, t, J = 6.8 Hz, 2pyH^{3,5}), 2.91 (24 H, s, $8NH_3$). Anal. Calcd (%) for $C_{34}H_{52}F_{36}N_{16}P_6Ru_2\cdot 0.5Me_2CO\cdot H_2O$: C, 23.64; H, 3.18; N, 12.42. Found: C, 23.38; H, 3.17; N, 12.04. Note: a small amount of **6** mixed with what appeared to be its asymmetric isomer based on ^{1}H NMR spectroscopy (15 mg) was collected before the main fraction of **6**.

Synthesis of [{*trans*-Ru^{II}(NH$_3$)$_4$(py)}$_3$Bbpypz][PF$_6$]$_8$ (7). This compound was prepared and purified in manner similar to **4**, by using *trans*-[Ru^{II}(NH$_3$)$_4$(py)(H$_2$O)][PF$_6$]$_2$ (200 mg, 0.360 mmol) and refrigeration for 1 h to afford a dark blue solid: 135 mg, 78%; δ_H (400 MHz, $(CD_3)_2CO$) 10.20 (2 H, s, $C_4H_2N_2$), 9.83 (4 H, d, J = 7.1 Hz, C_5H_4N), 9.25 (4 H, d, J = 6.8 Hz, C_5H_4N), 9.03 (2 H, d, J = 5.3 Hz, pyH^{2,6}), 8.98 (4 H, d, J = 7.1 Hz, C_5H_4N), 8.95 (4 H, d, J = 5.3 Hz, 2pyH^{2,6}), 8.21−8.13 (5 H, C_5H_4N + pyH^4), 8.02 (2 H, t, J = 7.8 Hz, 2pyH^4), 7.78 (2 H, t, J = 6.9 Hz, pyH^{3,5}), 7.64 (4 H, t, J = 6.9 Hz, 2pyH^{3,5}), 3.09 (12 H, s, $4NH_3$), 2.91 (24 H, s, $8NH_3$). Anal. Calcd (%) for $C_{39}H_{69}F_{48}N_{21}P_8Ru_3\cdot Me_2CO\cdot 3H_2O$: C, 20.96; H, 3.39; N, 12.22. Found: C, 21.04; H, 3.01; N, 12.22.

Hyper-Rayleigh Scattering. Details of the hyper-Rayleigh scattering (HRS) experiment have been discussed elsewhere,[12] and the experimental procedure used was as previously described.[13] β values were determined by using the electric-field-induced SHG β_{1064} value for 4-nitroaniline (29.2×10^{-30} esu in acetonitrile)[14] as an external reference. All measurements were performed by using the 1064 nm fundamental of an injection-seeded, Q-switched Nd^{3+}:YAG laser (Quanta-Ray GCR-5, 8 ns pulses, 7 mJ, 10 Hz). Dilute acetonitrile solutions (10^{-5}−10^{-6} M) were used to ensure a linear dependence of $I_{2\omega}/I_\omega^2$ on solute concentration, precluding the

(12) (a) Clays, K.; Persoons, A. *Phys. Rev. Lett.* **1991**, *66*, 2980. (b) Clays, K.; Persoons, A. *Rev. Sci. Instrum.* **1992**, *63*, 3285. (c) Hendrickx, E.; Clays, K.; Persoons, A.; Dehu, C.; Brédas, J.-L. *J. Am. Chem. Soc.* **1995**, *117*, 3547. (d) Hendrickx, E.; Clays, K.; Persoons, A. *Acc. Chem. Res.* **1998**, *31*, 675.

(13) Houbrechts, S.; Clays, K.; Persoons, A.; Pikramenou, Z.; Lehn, J.-M. *Chem. Phys. Lett.* **1996**, *258*, 485.

(14) Stähelin, M.; Burland, D. M.; Rice, J. E. *Chem. Phys. Lett.* **1992**, *191*, 245.

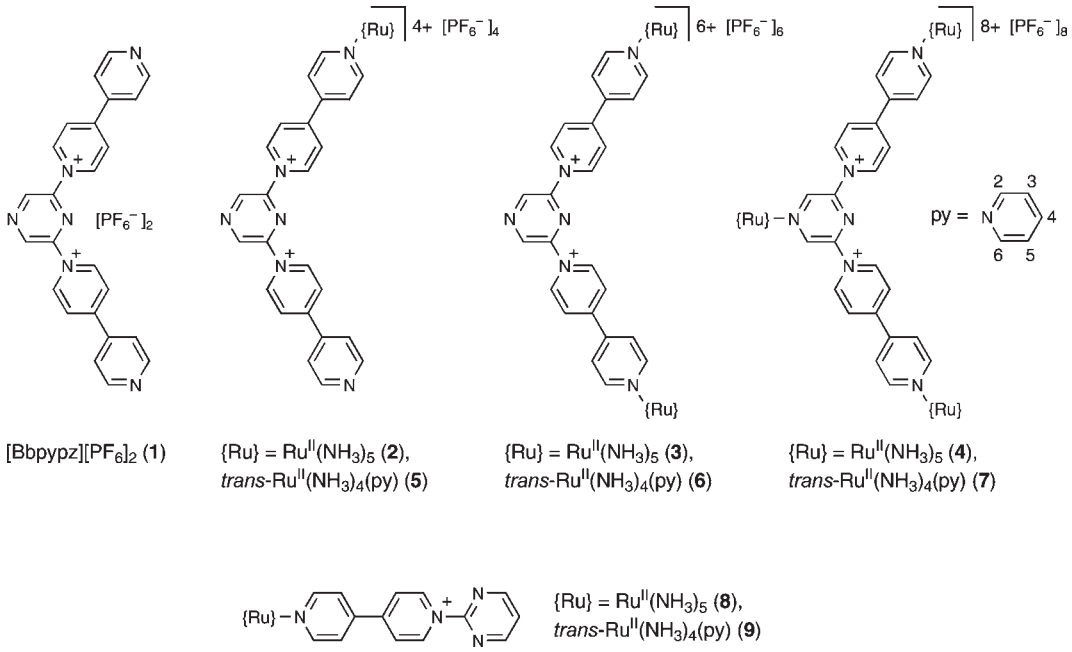

Figure 1. Chemical structures of the pro-ligand salt and complex salts investigated, and the previously reported 1D species,[8a] including the ^{1}H NMR labeling for the pyridine ligands.

need for Lambert−Beer correction factors. Samples were filtered (Millipore, 0.45 μm), and none showed any luminescence. HRS depolarization ratios[15] were determined at 1064 nm according to a published methodology.[16]

Stark Spectroscopy. The Stark apparatus, experimental methods, and data collection procedure were as previously reported,[17] except that a Xe arc lamp was used as the light source instead of a W filament bulb. The Stark spectrum for each compound was measured at least twice. The data analysis was carried out as previously described,[17] by using the zeroth, first and second derivatives of the absorption spectrum for analysis of the Stark $\Delta\varepsilon(\nu)$ spectrum in terms of the Liptay treatment.[18] The dipole-moment change, $\Delta\mu_{12} = \mu_e - \mu_g$, where μ_e and μ_g are the respective excited and ground-state dipole moments, was then calculated from the coefficient of the second derivative component. Butyronitrile was used as the glassing medium, for which the local field correction f_{int} is estimated as 1.33.[17] A two-state analysis of the MLCT transitions gives

$$\Delta\mu_{ab}^2 = \Delta\mu_{12}^2 + 4\mu_{12}^2 \quad (1)$$

where $\Delta\mu_{ab}$ is the dipole-moment change between the diabatic states and $\Delta\mu_{12}$ is the observed (adiabatic) dipole-moment change. The value of μ_{12} can be determined from the oscillator strength f_{os} of the transition by

$$|\mu_{12}| = \left(\frac{f_{os}}{1.08 \times 10^{-5} E_{max}}\right)^{1/2} \quad (2)$$

where E_{max} is the energy of the ICT maximum (in wavenumbers) and μ_{12} is in eÅ. The latter is converted into Debye units upon multiplying by 4.803. The degree of delocalization c_b^2 and electronic coupling matrix element H_{ab} for the diabatic states are given by

$$c_b^2 = \frac{1}{2}\left[1 - \left(\frac{\Delta\mu_{12}^2}{\Delta\mu_{12}^2 + 4\mu_{12}^2}\right)^{1/2}\right] \quad (3)$$

$$|H_{ab}| = \left|\frac{E_{max}(\mu_{12})}{\Delta\mu_{ab}}\right| \quad (4)$$

If the hyperpolarizability β_0 tensor has only nonzero elements along the MLCT direction, then this quantity is given by

$$\beta_0 = \frac{3\Delta\mu_{12}(\mu_{12})^2}{(E_{max})^2} \quad (5)$$

A relative error of ±20% is estimated for the β_0 values derived from the Stark data and using eq 5, while experimental errors of ±10% are estimated for μ_{12}, $\Delta\mu_{12}$, and $\Delta\mu_{ab}$, ±15% for H_{ab}, and ±50% for c_b^2. Note that the ±20% uncertainty for the β_0 values is merely statistical and does not account for any errors introduced by two-state extrapolation.

Results and Discussion

Synthetic Studies. The synthesis of the pro-ligand salt 2,6-bis(4′-pyridyl-1′-pyridiniumyl)pyrazine hexafluorophosphate, [Bbpypz][PF$_6$]$_2$ (**1**) (Figure 1), was based on the published method for the corresponding chloride salt.[9] The ruthenium complex salts (Figure 1) were prepared by reacting **1** with either [Ru^{II}(NH$_3$)$_5$(H$_2$O)][PF$_6$]$_2$[10] or *trans*-[Ru^{II}(NH$_3$)$_4$(py)(H$_2$O)][PF$_6$]$_2$[11] in acetone. While the crude yields of these reactions are high, separation of the mono and bis-Ru complexes requires column chromatography, using mixtures of aqueous NaCl and acetone on Sephadex CM-25 resin. Subsequent reprecipitations with aqueous

(15) Heesink, G. J. T.; Ruiter, A. G. T.; van Hulst, N. F.; Bölger, B. *Phys. Rev. Lett.* **1993**, *71*, 999.
(16) (a) Hendrickx, E.; Boutton, C.; Clays, K.; Persoons, A.; van Es, S.; Biemans, T.; Meijer, B. *Chem. Phys. Lett.* **1997**, *270*, 241. (b) Boutton, C.; Clays, K.; Persoons, A.; Wada, T.; Sasabe, H. *Chem. Phys. Lett.* **1998**, *286*, 101.
(17) (a) Shin, Y. K.; Brunschwig, B. S.; Creutz, C.; Sutin, N. *J. Phys. Chem.* **1996**, *100*, 8157. (b) Coe, B. J.; Harris, J. A.; Brunschwig, B. S. *J. Phys. Chem. A* **2002**, *106*, 897.
(18) (a) Liptay, W. In *Excited States*; Lim, E. C., Ed.; Academic Press: New York, 1974; Vol. *1*, pp 129−229. (b) Bublitz, G. U.; Boxer, S. G. *Annu. Rev. Phys. Chem.* **1997**, *48*, 213. (c) Vance, F. W.; Williams, R. D.; Hupp, J. T. *Int. Rev. Phys. Chem.* **1998**, *17*, 307. (d) Brunschwig, B. S.; Creutz, C.; Sutin, N. *Coord. Chem. Rev.* **1998**, *177*, 61.

Table 1. Selected ^{1}H NMR Data for the Pro-Ligand Salt **1** and Complex Salts **2**−**9**[a]

salt	$C_4H_2N_2$ singlets		C_5H_4N doublets										NH_3 singlets	
1	10.15		10.12	9.04	8.97	8.17								
2	10.13[b]		10.11	9.92	9.29	9.05	9.01	8.96	8.15	8.02	3.91	2.82		
3	10.05		9.89	9.28	8.99	8.01					3.86	2.78		
4	10.15		9.67	9.26	8.90	7.96					4.36	3.86	2.94	2.80
5	10.15	10.11	10.13	10.01	9.27	9.07−9.03[c]	8.98−8.94[d]	8.21	8.16		2.92			
6	10.09		10.00	9.27	9.04	8.22					2.91			
7	10.20		9.83	9.25	8.98	8.21−8.13[d]					3.09	2.91		
8[e]			10.17	9.28−9.22[f]	8.94	8.03−7.96[f]					3.75	2.74		
9[e]			10.28	9.26	8.99−8.93[d]	8.19					2.88			

[a] Spectra recorded in $(CD_3)_2CO$, at 400 MHz for **1**−**7** and at 200 MHz for **8** and **9**; all values are given in ppm with respect to TMS. [b] Signal consists of two singlets, separated by only about 0.003 ppm (1 Hz). [c] Two overlapped C_5H_4N signals. [d] Overlapped with a py ligand signal. [e] Data taken from ref 8a. [f] Overlapped with a $C_4H_3N_2$ signal.

NH_4PF_6 afforded the PF_6^- salts **2**, **3**, and **5** in moderate yields of about 20−30%, while **6** was isolated in only 10% yield following a final reprecipitation from acetone/diethyl ether. By contrast, the tris-Ru complex salts **4** and **7** were obtained pure without chromatography in high yields of 63 and 78%, respectively, by treating **1** with 5−6 equiv of the appropriate Ru^{II} aquo complex. The yields are always significantly higher for the *trans*-$\{Ru^{II}(NH_3)_4(py)\}^{2+}$ complexes when compared with their $\{Ru^{II}(NH_3)_5\}^{2+}$ counterparts (note that a substantial amount of **6** was lost upon reprecipitation from acetone/diethyl ether), despite using larger relative quantities of the pentaammine precursor. These observations appear to contradict the reported increased relative lability of the aquo ligand in $[Ru^{II}(NH_3)_5(H_2O)]^{2+}$,[19] but may be attributable to facile oxidative decomposition of this complex prior to reaction with $Bbpypz^{2+}$.

As expected, the pyridyl N atoms of **1** coordinate more readily than the 4-pyrazine N atom. This effect is attributable to the inherently lower basicity of pyrazine when compared with pyridine (py), and also the presence of the proximal positive charges. The symmetric species **3** and **6** can thus be prepared in preference to their asymmetric isomers, although a small amount of the asymmetric isomer of **6** was apparently detected via ^{1}H NMR spectroscopy (see above). In the previously published study with $[Bbpypz]Cl_2$, coordination of Cu^{II} centers was observed only at the pyridyl sites.[9] However, Ru^{II} coordination at the pyrazinyl (pz) N atom does occur efficiently at room temperature, provided that sufficient Ru^{II} aquo precursor complex is present. It is likely that this complexation behavior is facilitated by strong π-back-bonding interactions with the electron deficient ligand system.

The identities and purities of the new compounds are confirmed by diagnostic ^{1}H NMR spectra together with elemental analyses. The latter indicate that all of the PF_6^- salts are hydrated, as is often the case for Ru^{II} ammine species. In addition, **4**, **6**, and **7** also retain small quantities of acetone, as confirmed by ^{1}H NMR spectroscopy. The samples were not rigorously dried before making measurements to avoid any decomposition. Ru^{II} ammine complex salts do not generally give informative mass spectra, and despite many attempts, the new compounds showed typical behavior. Both ES^+ and MALDI measurements reveal only clearly identified peaks for the pro-ligand at m/z = 535.2 ($[\mathbf{1} - PF_6)]^+$) and 195.1 ($[\mathbf{1} - 2PF_6]^{2+}$), together with several unidentifiable peak envelopes with Ru-containing isotope patterns.

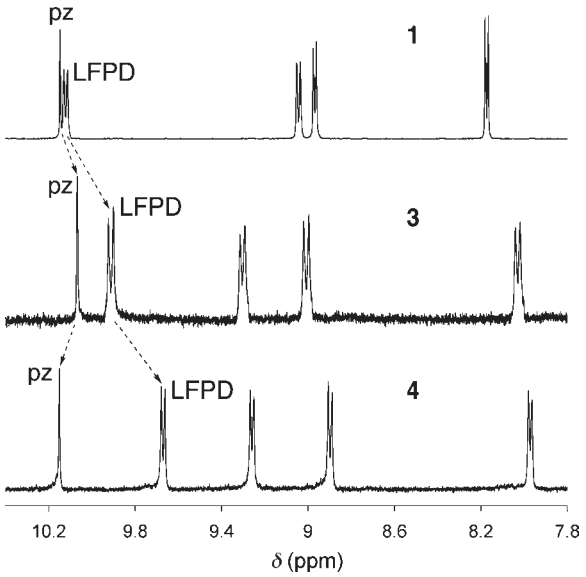

Figure 2. Aromatic regions of the ^{1}H NMR spectra for the pro-ligand salt **1** and the complex salts **3** and **4** recorded at 400 MHz in $(CD_3)_2CO$ at 293 K.

^{1}H NMR Spectroscopy Studies. Data for the signals associated with the protons of the pz, pyridyl, and NH_3 groups are collected in Table 1, together with data for **8** and **9**[8a] for comparison purposes. Representative spectra for salts **1**, **3**, and **4** are shown in Figure 2.

The asymmetric mono-Ru and symmetric bis-Ru complexes are readily distinguished by their number of proton signals as well as the integrals for the signals associated with the NH_3 and py ligands. In the tris-Ru complexes, the addition of a third Ru^{II} center in a non-equivalent position results in extra NH_3 signals that are shifted noticeably downfield by the electron-poor pz ring. For **4**, the two signals for the axial NH_3 ligands are separated by 0.5 ppm, while the difference for the equatorial NH_3 signals is rather smaller at 0.14 ppm (Table 1), showing that the ligands located trans to the *N*-heterocycle are more sensitive to its structure. Coordination of a third Ru center also causes the pz proton signals to shift downfield by about 0.1 ppm when compared to the bis-Ru complexes (Figure 2). The pz-coordinated Ru^{II} ammine moieties therefore exert a net deshielding influence on the 3,5-positions of the pz rings. In contrast, coordination of two Ru^{II} centers to the pyridyl

(19) Isied, S. S.; Taube, H. *Inorg. Chem.* **1976**, *15*, 3070.

Table 2. UV−vis Absorption and Electrochemical Data for Complex Salts **2**−**9** in Acetonitrile

				E, V vs Ag−AgCl (ΔE_p, mV)[b]	
salt	λ_{max}, nm (ε, 10^3 M^{-1} cm^{-1})[a]	E_{max} (eV)	assignment	oxidations, $E_{1/2}$	reductions, $E_{1/2}$ or E_{pc}
2	707 (17.7)	1.75	d → π^* (bpy)	0.54 (100)	−0.24 (110)[c]
	288 (32.6)	4.31	$\pi \rightarrow \pi^*$		−0.42 (90)[c]
3	713 (30.3)	1.74	d → π^* (bpy)	0.54 (110)	−0.27 (140)[c]
	285 (32.6)	4.35	$\pi \rightarrow \pi^*$		−0.45 (110)[c]
4	711 (30.0)	1.74	d → π^* (bpy)	0.55 (110)	−0.30 (120)[c]
	459 (10.3)	2.70	d → π^* (pz)	1.02 (260)	−0.45 (90)[c]
	287 (33.5)	4.32	$\pi \rightarrow \pi^*$		
5	675 (17.6)	1.84	d → π^* (bpy)	0.71 (80)	−0.21 (120)
	379 (7.3)	3.27	d → π^* (py)		−0.43[d]
	288 (38.0)	4.31	$\pi \rightarrow \pi^*$		
6	674 (31.1)	1.84	d → π^* (bpy)	0.71 (80)	−0.22 (90)[c]
	384 (12.4)	3.23	d → π^* (py)		−0.40 (70)[c]
	285 (33.6)	4.35	$\pi \rightarrow \pi^*$		
7	665 (32.2)	1.86	d → π^* (bpy)	0.73 (100)	−0.23 (110)[c]
	465 (17.2)	2.67	d → π^* (pz)	1.13 (170)	−0.39 (100)[c]
	382 (16.4)	3.25	d → π^* (py)		
	282 (42.2)	4.40	$\pi \rightarrow \pi^*$		
8[e]	673 (18.0)	1.84	d → π^* (bpy)	0.54 (100)	−0.40 (200)[c]
	285 (21.5)	4.35	$\pi \rightarrow \pi^*$		
9[e]	644 (16.8)	1.93	d → π^* (bpy)	0.72 (80)	−0.36 (90)[c]
	385 (5.8)	3.22	d → π^* (py)		−1.05 (100)[c]
	283 (24.5)	4.38	$\pi \rightarrow \pi^*$		

[a] Solutions about $5-9 \times 10^{-5}$ M. [b] Solutions about 10^{-3} M in analyte and 0.1 M in $[N(C_4H_9\text{-}n)_4]PF_6$ at a 2 mm disk glassy carbon working electrode with a scan rate of 200 mV s^{-1}. Ferrocene internal reference $E_{1/2}$ = 0.46 V, ΔE_p = 70−90 mV. [c] Irreversible reduction process ($i_{pc} > i_{pa}$). [d] E_{pc} for an irreversible reduction. [e] Data taken from ref 8a (all conditions as for **2**−**7**, except that a Pt-bead working electrode was used for the cyclic voltammetry).

groups of **1** causes the lowest field pyridyl doublet (LFPD) signal, associated with the protons located adjacent to the pyridinium N atoms, to shift upfield by 0.23 ppm in **3** (Figure 2) and by 0.12 ppm in **6**. The other three doublets show downfield shifts on bimetallic complexation, except for the highest field signal in **3** that shifts upfield. The coordination of a third Ru^{II} center to the pz N atom induces further, substantial upfield shifts in the LFPD signal of 0.22 ppm in **4** (Figure 2) and 0.17 ppm in **7**, while the other doublets show only small upfield shifts. These observations confirm that the LFPD signal is associated with the 2,6-protons of the pyridinium rings. Logically, the more strongly electron donating $\{Ru^{II}(NH_3)_5\}^{2+}$ moiety gives rise to relatively larger shifts when compared with *trans*-$\{Ru^{II}(NH_3)_4(py)\}^{2+}$.

Comparisons with the data for the previously reported complex salts (Table 1) show that the LFPD signal in **2**−**4** is shielded by 0.06−0.4 ppm with respect to that in **8**, and the same is true of **5**−**7** when compared with **9** (range 0.15−0.45 ppm). These differences can be attributed to the stronger relative electron-withdrawing influence of a 2,6-diazoaryl ring when compared with its 2,5-counterpart. In contrast, the NH_3 protons appear to experience small relative *deshielding* effects in the new compounds when compared with **8** and **9**.

Electronic Spectroscopy Studies. The UV−vis absorption spectra of complex salts **2**−**7** were recorded in acetonitrile, and the results are presented in Table 2, together with data for **8** and **9**[8a] for comparison purposes. Representative spectra of **2**−**5** are shown in Figure 3. All of the spectra show two strong bands, comprising one low-energy absorption associated with d(Ru^{II}) → π^*(bpy) (bpy = 4,4′-bipyridyl) MLCT transitions, and a higher energy band assigned to ligand-based $\pi \rightarrow \pi^*$ transitions. Additional, weaker MLCT absorptions due to Ru^{II} → py MLCT (in **5**−**7**) or Ru^{II} → pz excitations (in **4** and **7**) are observed between the two dominant bands.

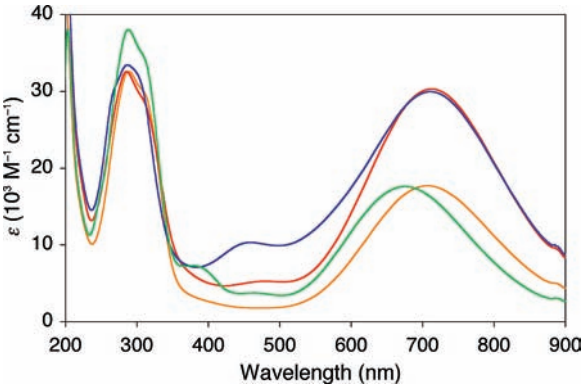

Figure 3. Electronic absorption spectra of **2** (orange), **3** (red), **4** (blue), and **5** (green) at 293 K in acetonitrile.

The dominant MLCT band shows blue shifts, corresponding with increases in E_{max} of about 0.1 eV, on replacing axial NH_3 ligands with py. This effect is largely due to increased stabilization of the Ru-based highest occupied molecular orbital (HOMO), and has also been noted in previous studies with 1D Ru^{II} ammine chromophores.[8a,20] However, this structural change does not affect the band intensities significantly. Increasing the number of Ru centers from one to two has little or no effect on the MLCT E_{max}, but logically almost doubles ε. Moving along the *trans*-$\{Ru^{II}(NH_3)_4(py)\}^{2+}$ series **5**−**7**, ε for the Ru^{II} → py MLCT band also increases steadily. Coordinating a third Ru center does not affect the main MLCT transition to any great extent. The energy separation of about 0.6 eV between the Ru^{II} → py and Ru^{II} → pz MLCT bands in **7** is

(20) Coe, B. J.; Jones, L. A.; Harris, J. A.; Brunschwig, B. S.; Asselberghs, I.; Clays, K.; Persoons, A.; Garín, J.; Orduna, J. *J. Am. Chem. Soc.* **2004**, *126*, 3880.

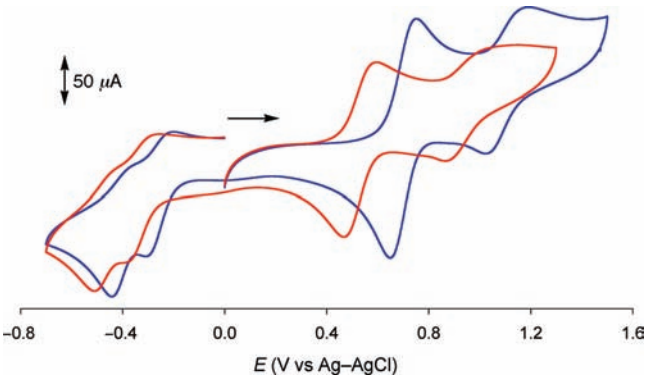

Figure 4. Representative cyclic voltammograms of the trimetallic complex salts **4** (red) and **7** (blue) at 293 K in acetonitrile (glassy-carbon disk working electrode, scan rate = 200 mV s^{-1}). The single-headed arrow indicates the direction of the initial scans.

attributable to the large difference in π-accepting abilities of the two heterocyclic units. The $Ru^{II} \rightarrow$ bpy MLCT E_{max} values for **2**−**4** are lower than that for **8** by about 0.1 eV, and the same applies to **5**−**7** when compared with **9**. In contrast, the $Ru^{II} \rightarrow$ py band energy shows less variation between the new and the previously published compounds. As expected, the ε values for the main MLCT band in the monometallic complexes in the pairs **2**/**8** and **5**/**9** are indistinguishable. The position and intensity of the high energy intraligand $\pi \rightarrow \pi^*$ band do not vary greatly within the series **2**−**4** and **5**−**7**, but these absorptions for **8** and **9** are considerably weaker when compared with the new species, because of the larger number of aryl rings in the latter.

Electrochemical Studies. Cyclic voltammograms of complex salts **2**−**7** were recorded in acetonitrile, and the resulting data are included in Table 2; all potentials are quoted with respect to the Ag−AgCl reference electrode. The previously published data for **8** and **9**[8a] are also included for comparison purposes, and representative voltammograms of **4** and **7** are shown in Figure 4.

All of the new compounds show reversible or quasi-reversible oxidations of the pyridyl-coordinated ruthenium center(s), with an $E_{1/2}$ value of about 0.55 V for the $\{Ru^{II}(NH_3)_5\}^{2+}$ systems **2**−**4** and about 0.72 V for the *trans*-$\{Ru^{II}(NH_3)_4(py)\}^{2+}$ species **5**−**7**. These observations are consistent with the expected HOMO stabilization in the latter complexes,[8a,20] and correlate with the MLCT energies (see above). The $Ru^{III/II}$ $E_{1/2}$ values for **2**−**4** are indistinguishable from that for **8**, while the same is true for **5**−**7** and **9**, showing that exchanging a 2-pyrimidyl for a 2-pyrazinyl *N*-substituent has no effect on the HOMO energy. Therefore, the small red shifts in the MLCT bands observed on moving from **8** to **2**−**4** or from **9** to **5**−**7** (see above) are attributable to stabilization of the ligand-based lowest unoccupied molecular orbital (LUMO). The fact that each of **3** and **6** displays only a single $Ru^{III/II}$ wave shows that the two metal centers in these compounds do not interact appreciably in an electronic sense; this observation is in keeping with the almost constant MLCT E_{max} values for the pairs **2**/**3** and **5**/**6**, and is unsurprising given that the Ru ions are separated by five aryl rings. The trimetallic systems show a second $Ru^{III/II}$ wave associated with the pyrazine-coordinated Ru^{II} center, at $E_{1/2}$ = 1.02 V for **4** and 1.13 V for **7**. These waves show ΔE_p values considerably larger than those of the other $Ru^{III/II}$ processes, indicating a lower degree of electrochemical reversibility.

All six compounds show two ligand-based reduction processes, that are not properly reversible, with "$E_{1/2}$" values in the ranges −(0.21−0.30) V and −(0.39−0.45) V. In all cases except for **5**, the return waves are weak and poorly defined. For **5**, a strong return wave is seen for the first reduction, but none for the second. Given the lack of true reversibility, it is inappropriate to comment in detail on the measured potentials. However, it should be noted that the substantial increases in the first ligand reduction potential (by 100 mV or more) for **2**−**4** when compared with **8** and for **5**−**7** when compared with **9** confirm the relative LUMO stabilization in the new species (see above), attributable to increased charge delocalization because of the presence of two extra aryl rings.

HRS Studies. The β values of complex salts **2**−**7** have been measured in acetonitrile solutions by using the HRS technique[12,13] with a 1064 nm Nd^{3+}:YAG laser, and the results are shown in Table 3. This laser wavelength was chosen because all of the compounds show MLCT absorption maxima well above the second harmonic (SH) wavelength of 532 nm (Table 2). The hyperpolarizability data shown are orientationally averaged $(\langle\beta^2_{HRS}\rangle)^{1/2}$ values derived from the total HRS intensity, regardless of molecular symmetry. Because all of the new compounds show only a single low energy MLCT band, we have used the two-state model[21] and the λ_{max} values (Table 2) to derive estimated β_0 values; the results are included in Table 3. The previously published data for **8** and **9**[8a] are also included for comparison purposes.

The new chromophores, especially the bi/trimetallic ones, are not simple two-state systems, so the estimated β_0 values should be treated with caution. Nevertheless, these data do show a clear and reasonable trend of increasing as the number of Ru^{II} centers increases from 1 to 2, that is, on moving from **2** to **3** or from **5** to **6** (Table 3). Adding a third metal center possibly causes β_0 to decrease, consistent with the presence of directionally opposed MLCT transitions, while changing the trans ligands from NH_3 to py has no consistent effect. Notably, the related 1D systems **8** and **9** show effectively identical β_0 values, which are similar to those determined for the monometallic compounds **2** and **5**, but smaller than those of **3** and **6** (Table 3).

Because of their V-shaped molecular structures, the β responses of **2**−**7** are expected to have significant 2D character. A C_{2v} symmetric molecule has five nonzero components of the β tensor, β_{zzz}, β_{zyy}, β_{zxx}, β_{yyz}, and β_{xxz}. If Kleinman symmetry applies, $\beta_{zyy} = \beta_{yyz}$ and $\beta_{zxx} = \beta_{xxz}$, and if the structure is essentially 2D, then $\beta_{zxx} = \beta_{xxz} = 0$, so only β_{zzz} and β_{zyy} are significant. To derive "off-diagonal" tensor components, we have measured HRS depolarization ratios ρ for **2**−**7**, and these are included in Table 3. The parameter ρ is the ratio of the intensities of the scattered SH light polarized parallel and perpendicular to the polarization direction of the fundamental beam.[15] A ρ value of 5 is the upper limit for purely dipolar symmetry, corresponding with a single β_{zzz} tensor component, under ideal experimental conditions. The reference compound

(21) (a) Oudar, J. L.; Chemla, D. S. *J. Chem. Phys.* **1977**, *66*, 2664. (b) Oudar, J. L. *J. Chem. Phys.* **1977**, *67*, 446.

Table 3. HRS Data and Depolarization Ratios for Complex Salts **2**−**9** in Acetonitrile

salt	$(\langle\beta^2_{HRS}\rangle)^{1/2}$ [a] (10^{-30} esu)	β_0 [b] (10^{-30} esu)	ρ [c]	k	β_{zzz} [d] (10^{-30} esu)	β_{zyy} [d] (10^{-30} esu)
2	600 ± 40	257 ± 17	3.5 ± 0.3	2.3 ± 0.7	1450 ± 100	
3	765 ± 165	336 ± 72	2.3 ± 0.7	10 ± 3	125 ± 30	1240 ± 600
4	600 ± 100	261 ± 43	2.3 ± 0.5	10 ± 3	100 ± 15	975 ± 500
5	550 ± 50	200 ± 18	3.9 ± 0.4	1.7 ± 0.5	1330 ± 120	
6	900 ± 100	326 ± 36	3.7 ± 0.3	1.9 ± 0.6	680 ± 75	1290 ± 190
7	900 ± 100	309 ± 34	3.4 ± 0.3	2.4 ± 0.7	560 ± 65	1335 ± 240
8[e]	640 ± 95	230 ± 35				
9[e]	774 ± 115	228 ± 34				

[a] Orientationally averaged β without any assumption of symmetry or contributing tensor elements, measured by using a 1064 nm Nd^{3+}:YAG laser. The quoted cgs units (esu) can be converted into SI units ($C^3\,m^3\,J^{-2}$) by dividing by a factor of 2.693×10^{20}. [b] Static first hyperpolarizability estimated from $(\langle\beta^2_{HRS}\rangle)^{1/2}$ via the two-state model.[21] [c] Depolarization ratio. [d] β tensor components derived from the HRS intensity and depolarization ratio measurements by using eqs 6−8. [e] Data taken from ref 8a.

Disperse Red 1 typically gives a rather lower ρ value of about 3.5.

The values of β_{zzz} and β_{zyy} can be determined from $\langle\beta^2_{HRS}\rangle$ and ρ as follows:

$$\begin{cases} \langle\beta^2_{HRS}\rangle = \langle\beta^2_{ZZZ}\rangle + \langle\beta^2_{YZZ}\rangle \\ \rho = \dfrac{\langle\beta^2_{ZZZ}\rangle}{\langle\beta^2_{YZZ}\rangle} \end{cases} \tag{6}$$

The HRS intensities with parallel polarization for fundamental and SH wavelengths, $\langle\beta^2_{ZZZ}\rangle$, and for perpendicular polarization, $\langle\beta^2_{YZZ}\rangle$, are given in terms of the molecular tensor components β_{zzz} and β_{zyy} according to

$$\begin{cases} \langle\beta^2_{ZZZ}\rangle = \dfrac{1}{7}\beta^2_{zzz} + \dfrac{6}{35}\beta_{zzz}\beta_{zyy} + \dfrac{9}{35}\beta^2_{zyy} \\ \langle\beta^2_{YZZ}\rangle = \dfrac{1}{35}\beta^2_{zzz} - \dfrac{2}{105}\beta_{zzz}\beta_{zyy} + \dfrac{11}{105}\beta^2_{zyy} \end{cases} \tag{7}$$

and ρ can be expressed in terms of the parameter $k = \beta_{zyy}/\beta_{zzz}$ by

$$\rho = \frac{15 + 18k + 27k^2}{3 - 2k + 11k^2} \tag{8}$$

The ρ value decreases on moving from **2** to **3**, then remains unchanged for **4**. These observations are consistent with the more strongly 2D nature of the symmetric chromophores. However, this pattern is not repeated convincingly for **5**−**7** which have ρ values that are indistinguishable given the estimated experimental error limits.

For the asymmetric compounds **2** and **5**, the relatively high ρ values and the presence of only one electron donating Ru^{II} center indicate that the β_{zzz} tensor components dominate, so only these are reported. For the symmetric species, values of β_{zzz} and β_{zyy} have been derived by using eqs 6−8 (Table 3), showing that β_{zyy} dominates in all cases. No significant differences in the relative magnitude of the two tensor components (i.e., k) are observed between the related bi- and trimetallic species, but the relative contribution of β_{zyy} is larger in the $\{Ru^{II}(NH_3)_5\}^{2+}$ complexes **3** and **4** when compared with their *trans*-$\{Ru^{II}(NH_3)_4(py)\}^{2+}$ counterparts **6** and **7**. Since ρ measurements can give misleading results, because of resonance effects and Kleinman symmetry breaking,[5h,22] the quoted values of β_{zzz} and β_{zyy} for our new pyrazinyl species may be of limited accuracy. However, the HRS studies do clearly confirm the 2D nature of their β responses.

Stark Spectroscopic Studies. The complex salts **2**, **3**, **5**, and **6** have been studied by using Stark spectroscopy[18] in butyronitrile glasses at 77 K, and the results are presented in Table 4, together with data for **9**[17b] for comparison purposes (unfortunately, Stark data have not been reported for **8**). Representative absorption and electroabsorption spectra are shown in Figure 5. The trimetallic compounds were not studied because the presence of directionally opposed MLCT processes precludes meaningful application of the data obtained from Stark measurements to NLO responses.

The MLCT bands of **2**, **3**, **5**, and **6** show large red shifts of about 0.2 eV on moving from acetonitrile solutions to butyronitrile glasses (Tables 2 and 4), as also observed for other Ru^{II} ammine complex salts including **9**. The increases in the band intensities observed at room temperature on moving from mono- to bimetallic species are also reflected in the values of f_{os} and μ_{12} determined at 77 K. The parameter $\Delta\mu_{12}$ relates to a transition from a delocalized ground state, and affords r_{12}, the delocalized electron-transfer distance; these quantities are insensitive to the number of Ru^{II} centers, but both are larger for the *trans*-$\{Ru^{II}(NH_3)_4(py)\}^{2+}$ species **5** and **6** when compared with their $\{Ru^{II}(NH_3)_5\}^{2+}$ counterparts. This trend presumably reflects the increased molecular sizes caused by the py ligands. $\Delta\mu_{ab}$ refers to a transition from a localized ground state (i.e., corrected for the effects of metal−ligand bonding), while r_{ab} is the corresponding localized electron-transfer distance. In contrast with $\Delta\mu_{12}$ and r_{12}, $\Delta\mu_{ab}$ and r_{ab} increase on moving from mono- to bimetallic species. The greater relative size of the new compounds means that all of their $\Delta\mu$ and r values are larger than those determined previously for **9**.[17b] As for f_{os} and μ_{12}, the parameters c_b^2 and H_{ab} that quantify the degree of delocalization and π-electronic coupling are also enhanced by coordinating a second Ru^{II} center.

Given that effectively single, low energy MLCT bands are observed in all cases, we have used the standard two-state model[21,23] (i.e., eq 5, corresponding with the "perturbation series" convention) to estimate β_0 values from the Stark data; the results are included in Table 4. The

(22) Kaatz, P.; Shelton, D. P. *J. Chem. Phys.* **1996**, *105*, 3918.

(23) Willetts, A.; Rice, J. E.; Burland, D. M.; Shelton, D. P. *J. Chem. Phys.* **1992**, *97*, 7590.

Table 4. MLCT Absorption and Stark Spectroscopic Data for the Complex Salts **2**, **3**, **5**, **6**, **8**, and **9** in Butyronitrile at 77 K

salt	λ_{max} (nm)	E_{max} (eV)	f_{os}[a]	μ_{12}[b] (D)	$\Delta\mu_{12}$[c] (D)	$\Delta\mu_{ab}$[d] (D)	r_{12}[e] (Å)	r_{ab}[f] (Å)	c_b^2[g]	H_{ab}[h] (10^3 cm^{-1})	β_0[i] (10^{-30} esu)
2	790	1.57	0.19	5.7	16.4	19.9	3.4	4.2	0.09	3.6	252
3	790	1.57	0.51	9.3	16.3	24.7	3.4	5.2	0.17	4.8	662
5	742	1.67	0.21	5.7	19.4	22.5	4.0	4.7	0.07	3.4	259
6	742	1.67	0.63	10.0	19.4	27.9	4.0	5.8	0.15	4.8	816
9[j]	711	1.74	0.29	6.5	12.4	18.0	2.6	3.7	0.15	5.1	200

[a] Obtained from $(4.32 \times 10^{-9}$ M cm$^2)A$ where A is the numerically integrated area under the absorption peak. [b] Calculated from eq 2. [c] Calculated from $f_{int}\Delta\mu_{12}$ using $f_{int} = 1.33$. [d] Calculated from eq 1. [e] Delocalized electron-transfer distance calculated from $\Delta\mu_{12}/e$. [f] Effective (localized) electron-transfer distance calculated from $\Delta\mu_{ab}/e$. [g] Calculated from eq 3. [h] Calculated from eq 4. [i] Calculated from eq 5. [j] Data taken from ref 17b.

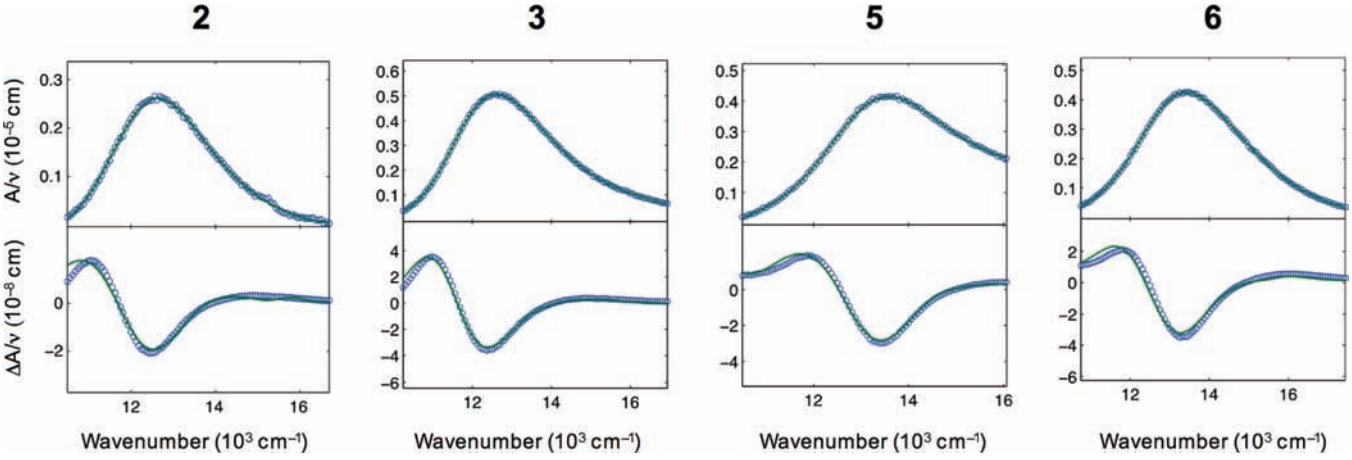

Figure 5. Stark spectra and calculated fits in an external electric field of 5.66×10^7 V m^{-1} for complex salts **2**, **3**, **5**, and **6**. Top panels: absorption spectrum; bottom panels: electroabsorption spectrum, experimental (blue) and fits (green) according to the Liptay equation.[18a]

validity of applying such an approximate approach to multidimensional systems has been discussed in detail previously.[24] The β_0 values show a clear trend of increasing by about 3-fold on moving from monometallic to bimetallic species, that is, **2** → **3** and **5** → **6**. Notably, the same pattern is evident in the HRS data (Table 3). These increases arise solely from the larger μ_{12} values for the bimetallics, since E_{max} and $\Delta\mu_{12}$ remain constant (Table 4). Comparisons with the β_0 value determined for **9** indicate that the new monometallic compounds **2** and **5** may have slightly larger responses, although the differences are within the estimated error limits (±20%). However, given that the HRS data also indicate such a trend, it is likely to be real. Finally, the Stark-based β_0 responses of **3** and **6** are very large and greater than those which we obtained for 1D and 2D monometallic Ru^{II} ammine complexes by using the same approach previously.[3i,7,8b,17b,20] By way of further comparison, a β_0 value of 236×10^{-30} esu was obtained for the benchmark salt [DAS]PF_6.[25]

Conclusions

We have synthesized and characterized the first family of NLO metallochromophores based on pyrazinyl cores. Their UV−vis absorption spectra are dominated by intense Ru^{II} → bpy MLCT bands, with only one maximum observed in the visible region for the pyridyl-coordinated complexes at room temperature in acetonitrile and at 77 K in butyronitrile. These absorptions remain at constant energy but gain intensity on increasing the number of Ru^{II} centers from one to two. The trimetallic species show an additional Ru^{II} → pz MLCT band to high energy. Cyclic voltammograms display a single reversible or quasi-reversible $Ru^{III/II}$ wave for the mono- and bimetallic complexes, with an irreversible oxidation wave appearing for the pyrazinyl-coordinated Ru in the trimetallic species. All of the ligand-based reduction processes are essentially irreversible. HRS studies with a 1064 nm laser show relatively large β values, and depolarization measurements confirm the strongly 2D nature of the NLO responses for the symmetric complexes, with dominant β_{zyy} tensor components. Stark spectroscopy affords estimated β_0 values that increase on moving from mono- to bimetallic species, in agreement with the HRS results. The enhanced MLCT intensities are the source of the greater NLO responses. The Stark-based β_0 values for the new bimetallic salts are larger than those determined for 1D and 2D monometallic Ru^{II} ammine complexes, and several times larger than that of [DAS]PF_6. The design strategy adopted is therefore very effective in creating highly active NLO chromophores with strongly 2D character.

Acknowledgment. We thank the EPSRC for support (Grants EP/E000738 and EP/D070732) and also the Fund for Scientific Research-Flanders (FWO-V, G.0312.08), the University of Leuven (GOA/2006/3), and the NSF (Grant CHE-0802907, "Powering the Planet: an NSF Center for Chemical Innovation"). I.A. is a postdoctoral fellow of the FWO-V.

(24) Coe, B. J.; Fielden, J.; Foxon, S. P.; Harris, J. A.; Helliwell, M.; Brunschwig, B. S.; Asselberghs, I.; Clays, K.; Garín, J.; Orduna, J. *J. Am. Chem. Soc.* **2010**, *132*, 10498.

(25) Coe, B. J.; Harris, J. A.; Asselberghs, I.; Wostyn, K.; Clays, K.; Persoons, A.; Brunschwig, B. S.; Coles, S. J.; Gelbrich, T.; Light, M. E.; Hursthouse, M. B.; Nakatani, K. *Adv. Funct. Mater.* **2003**, *13*, 347.